Calibration of *Chandra*'s Near On-Axis Performance

D. Jerius, T.J. Gaetz, and M. Karovska
Smithsonian Astrophysical Observatory, Cambridge MA 02138, USA

ABSTRACT

The Chandra X-Ray telescope has excellent angular resolution for on-axis sources. While its Wolter type I design optimizes on-axis performance, there is a relatively large region in which $0.5''$ to $1''$ imaging is possible. The Chandra PSF was first characterized during ground calibration and, most recently, from actual on-orbit measurements. The ground calibration provided data with the highest signal to noise but, because of gravity-induced distortions of the optics, could not completely characterize their performance. We present the results of on-orbit calibrations of the optics' performance, focusing on the near on-axis field of view. We present for the first time an analysis of the energy dependence of the on-orbit PSF.

Keywords: X-ray optics, PSF, Chandra

1. INTRODUCTION

The *Chandra* X-ray Observatory,[1] launched in 1999, has the best angular resolution of any astronomical X-ray telescope yet built, with optics capable of sub-arcsecond imaging. As such, it has enabled a staggering revolution in our knowledge of complex astrophysical systems, revealing structure on a range of scales and fundamentally changing our understanding of the physics underlying of both the small (AGN's, black holes) and the gigantic (clusters of galaxies). *Chandra*'s optical performance has enabled researchers to probe deep into systems where our knowledge of the physical processes depends upon answering a seemingly simple question: *Are the X-rays emitted from a compact, point-like region, or by a diffuse system?* In this regime, were the PSF many times oversampled, such a question would indeed by straightforward to resolve. There are, however, considerable detector and telescope artifacts which, coupled with at best a factor of two oversampling, complicate the analysis.

Calibration of *Chandra*'s mirrors (known as the High Resolution Mirror Assembly, or HRMA) was initially performed during ground testing at the X-ray Calibration Facility (XRCF) at Marshall Space Flight Center in Huntsville, Alabama, USA. The results were complicated by several effects:

- the optics were distorted by gravity
- the source was resolved (not a point)
- the source was at a finite distance, and thus not properly focused.
- the mirror shells were not tested as an ensemble at the same focus at all energies
- there was a limited set of X-ray energies

These, along with a tight constraint on the duration of the tests, precluded a thorough characterization of the PSF. Instead, the results were used to calibrate and validate a high-precision raytrace model of the optics. The model includes a finite-element model of the optics and their support structures, simulates their shape, surface characteristics, and coating, and implements a detailed facsimile of the baffles, and any obstructions in the

Further author information: (Send correspondence to D.J.); D.J.: E-mail: djerius@cfa.harvard.edu

optical path.[2] The model is the means of translating the optics' measured performance in the gravity distorted environment at the XRCF to the space environment for which they were designed.

The calibration measurements made at the XRCF provided us with a very high degree of confidence in the model and its predictions for the as-built, on-orbit performance of the optics. To verify this, measurements of the on-orbit PSF are required. Herein lies the rub; while the environment at the XRCF did not duplicate that in space, the X-ray source was strong and deterministic, and the detector systematics well understood and not significant distorters of the PSF. The on-orbit calibration relies upon serendipitous observations of sources whose flux is predominantly at lower energies, often variable, and, by necessity, low (in order not to overwhelm or destroy the science detectors).

2. ON-ORBIT CALIBRATION

Chandra's optics consist of a set of nested Wolter type I shells, each contributing an energy-dependent fraction of the total collecting area. A selection of sources with a wide range of energies is thus required to fully calibrate the PSF. Sources with flux at higher energies (> 4.5 keV) are especially valuable, as the innermost shell (with a known alignment error) is most easily separable from the others in this range. So far the on-orbit calibration of the PSF core has been done using observations of known point sources from the standard science program – there are no calibration-only observations specifically scheduled to study the core. As previously mentioned, on orbit work presents several challenges:

- There are few true on-axis "pointings" (telescope dither renders this somewhat meaningless, in any case).
- Telescope dither causes the object to be observed at a range of superimposed off-axis positions.
- Few point-like astrophysical sources have appreciable flux above 2 keV.
- The on-board science instruments have characteristics which hamper analysis of just the optics:
  - the HRC-I, a micro-channel plate detector, has no energy resolution
  - the HRC-I event position reconstruction introduces systematic offsets in recorded event positions
  - the other detector, ACIS, a CCD, has large pixels ($\sim 0.5''$).
  - ACIS uses both backside and frontside illuminated devices; the interaction of the photons with the pixel structure is thus different between them.
  - ACIS suffers from event pileup, so one must use very faint sources, or use it in conjunction with the high energy transmission grating (HETG), using the latter as a filter. One then analyzes the zero-order image, with the hope that this does not introduce unknown distortions to the PSF.

2.1. Known Deficiencies of the Telescope Model

While our model of the optics is fairly complete, the models of the ACIS detector and of the effects of telescope motion during the observation are primitive. Notwithstanding that the size of the ACIS pixel gate structure is on the same scale as the PSF, a pixel is treated as a featureless square bucket. Actual events are generally recorded as distributed across several pixels, as the charge cloud created by the interaction of the X-ray photon with the detector may spread across pixel boundaries. The spatial extent of the cloud is a function of energy as well. This undoubtedly alters the shape of the PSF; we do not model it.

As the telescope dithers, it moves the image across many pixels; over time the "core" of the PSF visits, fairly uniformly, every part of the pixel. This has little affect on observations made with the HRC-I, but because of the highly structured nature of CCDs, does affect ACIS observations. Our model is currently incapable of simulating this; we treat this by the addition of a uniform pixel-shaped blur to our raytraces. For ACIS, this ignores the interaction of the PSF with the pixel gate structure. The dither is actually rather slow, so that on short time scales the relative position of the PSF core within a pixel remains fairly constant. Depending upon the flux of the source, this could introduce systematic structure in the resultant image. There is another model of the telescope, MARX, which does simulate dither accurately, but it has a less accurate representation of the optics, and suffers from the same deficiencies in detector modeling.

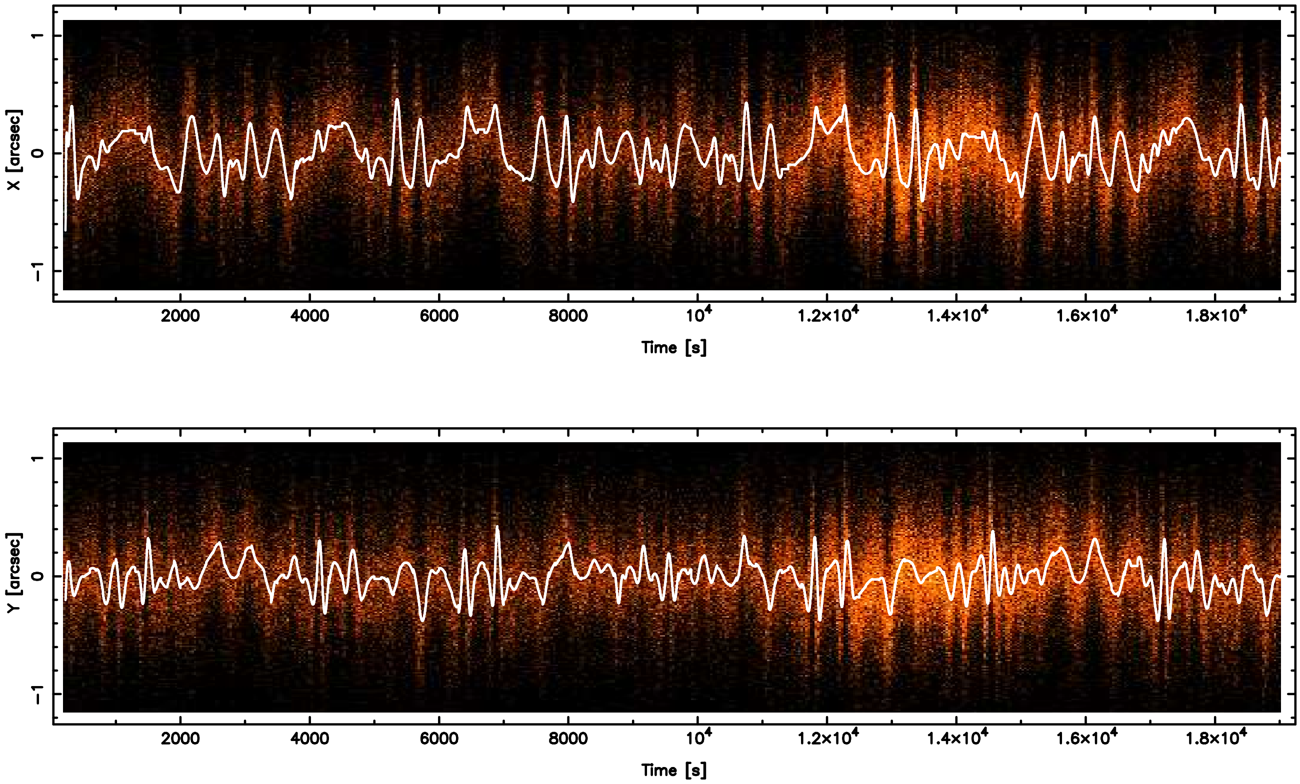

Figure 1. Motion of the image centroid in the HRC-I Observation of AR Lac. The curve is a piecewise continuous polynomial fit to the average event position.

2.2. Observations with the HRC-I

The observation made with the HRC-I which is most applicable to studies of the PSF is one of the star AR Lacertae (AR Lac) taken early in the mission (OBSID 1385). It was observed $0.29'$ off axis for $\sim$ 18.8ksec, resulting in $\sim$ 124000 events. An earlier analysis[3] indicated good agreement with models, but used a primitive approach to removing instrumental noise in the event positions. The noise is due to a detector artifact which causes shifts in the determined positions of events depending upon their position relative to the micro-channel plate's tiles.[4] The coupling of this behavior with telescope dither leads to an apparent motion of the image with time, even after the spacecraft aspect correction has been applied. This is illustrated in Fig. 1. The effect is not well enough understood to model it as part of our simulation, so we must remove its symptoms from the data. In the earlier work, we simply filtered out data at the extremes of the motion. Subsequent to that work we have improved our technique. We fit a set of essentially continuous piecewise polynomial functions to the data and subtract them. The spread of image centroids before and after the correction is shown in Fig. 2. To determine if the correction affects more than just the relative displacement of the image center, we applied a Kolmogorov-Smirnov test to the distributions of raw and corrected RMS event positions; it indicates that they are drawn from the same parent distribution. The RMS positions are shown in Fig. 3. A more detailed description of this analysis is available.[5]

We simulated HRC-I as a point source at the nominal off-axis pointing. As the HRC-I has no energy resolution, a spectrum of AR Lac (derived from other X-ray measurements) was applied to the point source, which was then imaged by the optics onto a model of a micro-channel plate detector. To simulate errors in the events' positions due to uncertainties in the telescope aspect reconstruction, we applied a Gaussian blur of $\sigma = 0.06''$.[6] We generated 1000 realizations of the observation to explore the systematics in the model.

We compare the simulations to the observational data by constructing radial profiles, shown in Fig. 4. The

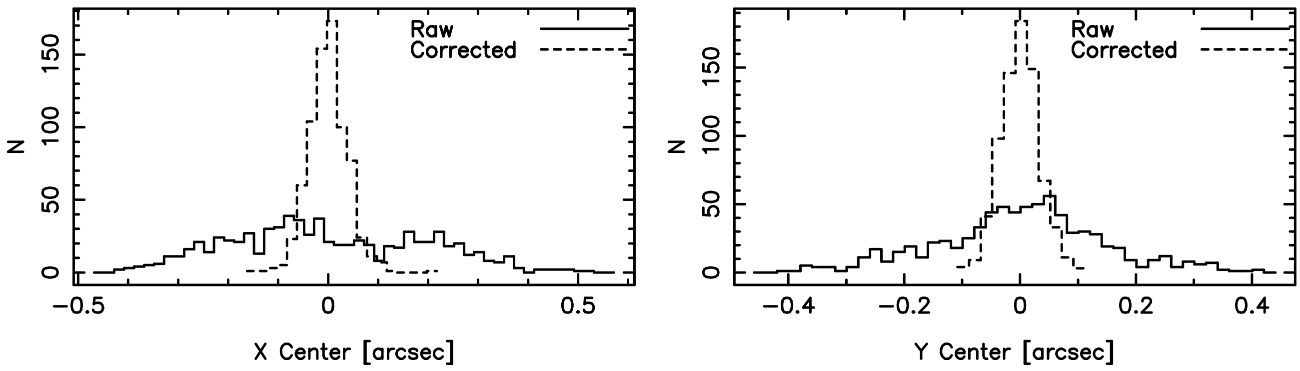

Figure 2. Distribution of image centroids (determined every 25 seconds) about the mean image center.

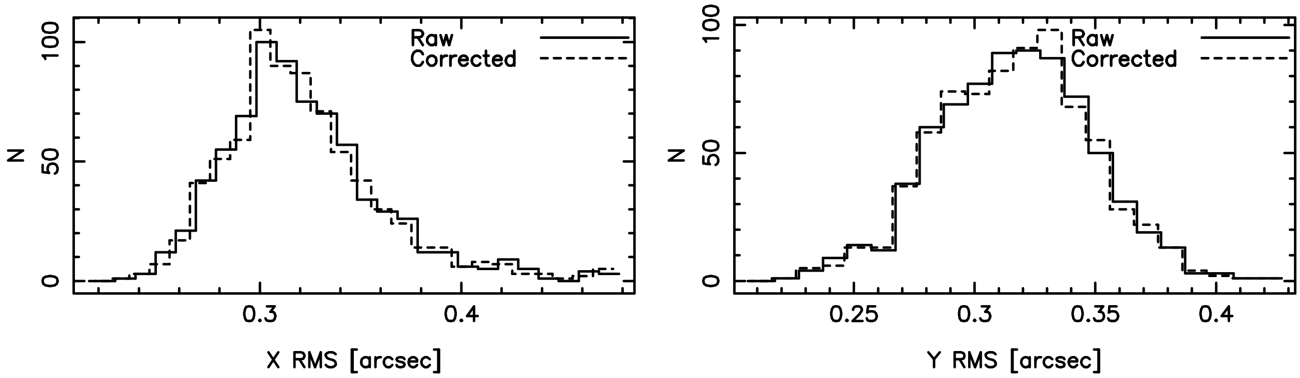

Figure 3. The distribution of the RMS of the event positions in 25 second time slices.

observational data have been background subtracted. The error bars bound 95% of the simulations. The model is clearly narrower than the observational data. A qualitative comparison of the two dimensional PSF is made in Fig. 5; the observational data show slightly different asymmetries, which may help explain the discrepancies, although overall the observational data appear to be more extended. Until we have improved our simulations of the telescope dither, we will not be able to determine the source of the discrepancies.

2.3. Observations with ACIS

ACIS has its own set of detector characteristics which enliven analysis. Events are detected using 3×3 pixel islands, and assigned "grades" based upon the pattern of pixels within the island whose charge exceeds a set value. Certain grades are known to most probably be the result of actual X-ray photons; events with those grades are kept. Most X-ray events at energies below 2 keV are predominantly grade 0 (*g0*); a single pixel contains all of the charge. Events at higher energies tend to be a mix of other grades, with grade 6 (*g6*), a grab bag of odd patterns, predominating. The amount of charge in the selected pixels in the island is representative of the energy of the photon.

If two or more photons are incident upon a pixel (or upon overlapping pixel islands) before the CCD frame is read out, they may be recorded as a single event. This is known as event pileup. Often the resultant event has a bad grade, and is rejected. Since pile up for a point source occurs at the peak of the surface brightness, this will result in an apparent decrease in brightness in the core of the PSF. If the piled up events result in a good grade, this represents a shift from the true grade (most likely *g0*); this is known as grade migration. Because these effects predominantly occur in the very core of the PSF, sources which exhibit them must be avoided.

We created an initial list of candidate point sources by selecting targeted observations classified as either "Normal Stars and White Dwarves" or "Black Hole and Neutron Star Binaries" by their principal investigators. We winnowed that list using several criteria designed to eliminate sources which were piled-up:

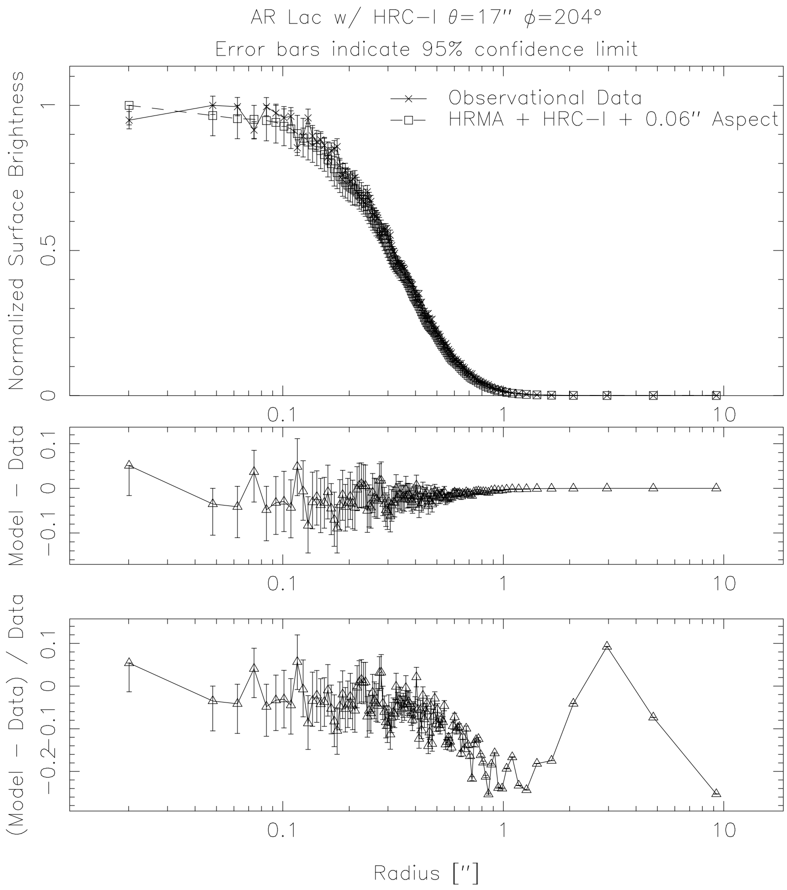

Figure 4. Radial profiles of the real and simulated AR Lac HRC-I observation

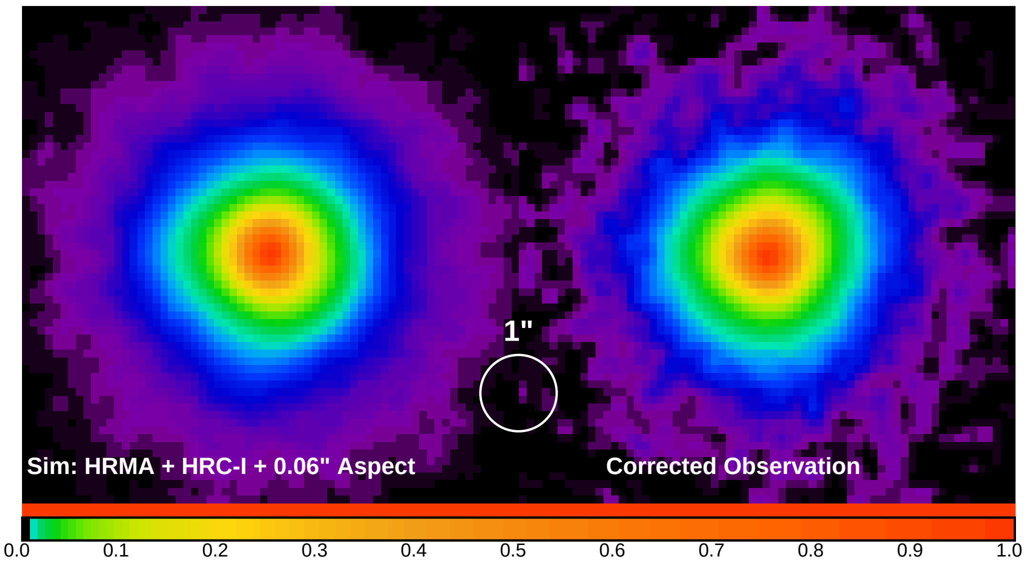

Figure 5. AR Lac: Simulated and corrected observations. The image is binned to ~ 1 HRC-I pixel. The observation shows somewhat more asymmetry than does the model.

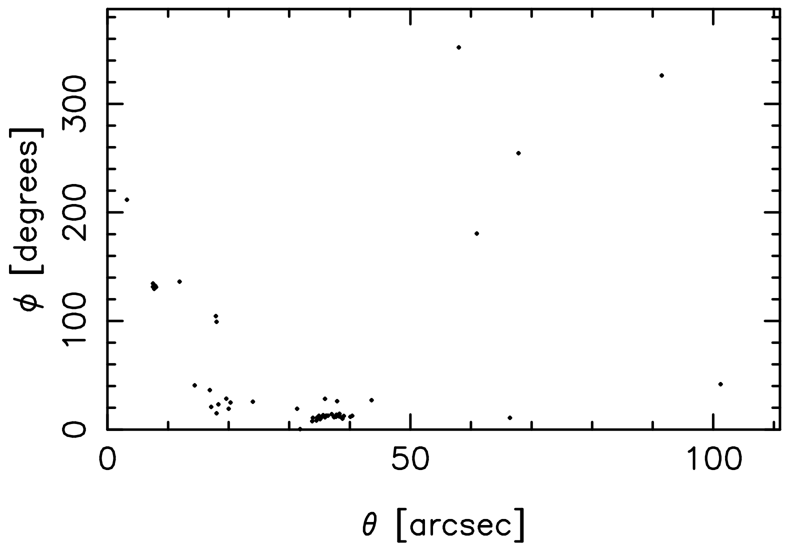

Figure 6. Distribution in the focal plane of sources observed with ACIS which are acceptable for analysis. θ is the off-axis angle; ϕ is the azimuthal angle.

- The ratio of event grades, in particular $g0/g6$, in the PSF core is a good indication of pileup. Piled up sources tend to have $g0/g6 \lesssim 1$, while non-piled up sources have $g0/g6 \gg 1$. Because event grades are also a function of energy, and higher energy events are less likely to be of grade 0, this criterion must be used with caution for objects with significant higher energy (> 2 keV) flux. The sources all had predominantly more flux below 2 keV, so by filtering out energies above 2 keV we eliminated the possible grade confusion without affecting the events most likely to be piled up.
- We examined the number of image frames where there was more than one event within 2 pixels of the nominal image center. Sources where more than $\sim 3\%$ of their frames met this limit were rejected.

The culling reduced the original number of objects from ~ 400 to 56. Of these, 7 were observed with ACIS-I (the primary imaging array within ACIS), 21 with ACIS-S (the sub-array used to image photons dispersed by the HETG), and 28 with ACIS-S + HETG. As the brightest of these has only ~ 10000 counts, coaddition of several observations was necessary to obtain a statistically relevant radial profile, in particular as we hoped to use the energy resolution of the device to diagnose the different mirror shells. This requires that the sources' positions relative to the telescope's optical axis be fairly similar; Fig. 6 shows their positions. Two separate pointings were extracted from this list, corresponding to the cluster near $\theta = 8''$ and a subset of the band with $30'' < \theta < 40''$. Table 1 indicates the average positions as well as the detectors used for the two pointings. Unfortunately, because some of these observations were still proprietary to the principal investigators at the time of this analysis, we are unable to publish more details on them. All of the observations are done with the ACIS-S, in particular using device S3, which is a backside illuminated CCD, and thus may introduce fewer artifacts into the PSF due to its gate structure. Of more concern is that most of the observations, including those with high energy flux, are imaged through the HETG, which may distort the PSF.

When the events are corrected by the standard data processing pipelines for telescope dither and relative motion between the detector and the optics, two steps are taken which result in distortion of the PSF when coadding observations performed with differing telescope rolls:

1. Events are transformed into a sky coordinate system based upon the standard astronomical right ascension and declination system. This involves rolling the observation about the telescope axis to account for the roll of the telescope at the time of the exposure.

Table 1. Mean off-axis distance (θ),azimuthal position (ϕ), detector, and counts, of coadded pointings

θ	ϕ	ACIS-S/HETG	ACIS-S	Counts
$7.7'' \pm 0.2$	$132° \pm 1.5$	7	0	48157
$35'' \pm 0.5$	$12° \pm 1.4$	5	3	68280

2. Events are randomized within pixels oriented to the astronomical coordinate system with sizes equal to the ACIS detector size.

The observations' aspect data were modified so that in the first step no roll would be performed. The pipeline was then rerun with sky pixel randomization turned off.

Unlike the HRC-I observation of AR Lac, ACIS detected events have energy information, so we do not need to know the astrophysical spectrum of the source to simulate the observations. We derived an input spectrum which exactly reproduces the detected spectrum after modification by the telescope optics and detectors. We imaged a point source with this spectrum with our optical model, and simulated the affects of dither and pixelization by:

1. randomizing a detected event within its corresponding ACIS pixel, in order to simulate the uncertain position of the event within a pixel ;
2. again randomizing within an ACIS pixel to simulate the effects of dither motion;
3. convolving the rays with a Gaussian of $\sigma = 0.06''$[6] to simulate aspect pointing errors.

As in the case of the HRC-I simulations, we generate 1000 realizations of the observation. The real and simulated events were divided into six subsets based upon their energies. Radial profiles were generated such that there were 400 events per radial bin.

Fig. 7 presents radial profiles for the $7.7''$ pointing, the closest to being on-axis. The error bars bound 95% of the simulations. A few things of note:

- As expected, the lack of flux beyond 2 keV leads to a paucity of data. There is only one included object with appreciable flux.
- The optics-only PSF is much narrower at lower energies than the observations. The discrepancies are probably due to insufficiencies in the models of the detector and dither, rather than in the model of the optics.
- The optics-only PSF is much broader at higher energies, and the contribution of the detector and dither models to discrepancies with the data are much less important.

While the overall shape of the modeled PSF is close to that observed, the discrepancies are disappointingly high, $\sim 10\%$. The behavior at low energies points to a flawed model for detectors and dither.

Fig. 8 presents a qualitative comparison of the two-dimensional PSF. The left column shows the optics-only model PSF compared with the observed data, while the right column compares the optics+detector+dither model PSF. Both data and model are binned at 0.1 ACIS pixels and smoothed with a 0.1 pixel Gaussian. This is done to illustrate the size of details in the model PSF and the effects of the detector and dither models on them; structures less than 0.5 pixels in the actual data are suspect. As expected from the radial profiles, the low energy model PSFs are dominated by the detector+dither model, and appear more symmetric than the observation. At high energies both model and data show an elongation, unfortunately in different directions. This is expected, and is thought to be due to a known alignment error in the innermost mirror shell, which is most sensitive to higher energies.

Figs. 9 and 10 present the same analysis for the $35''$ pointing. Again, a single object provides most of the flux above 2 keV. The conclusions are qualitatively the same as for the closer pointing. Of note is that the high

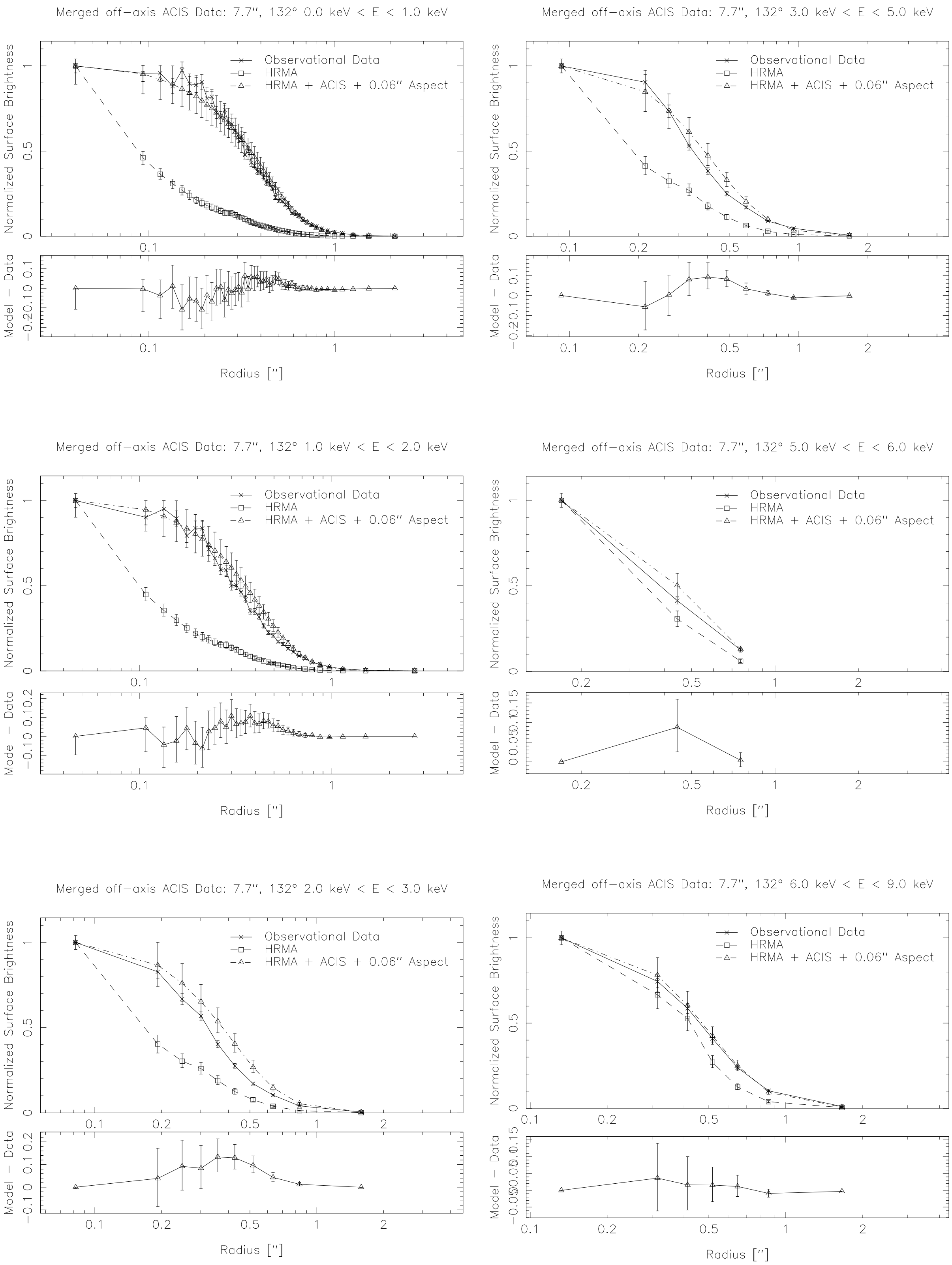

Figure 7. Comparisons of 1D PSFs for 7.7″ source.

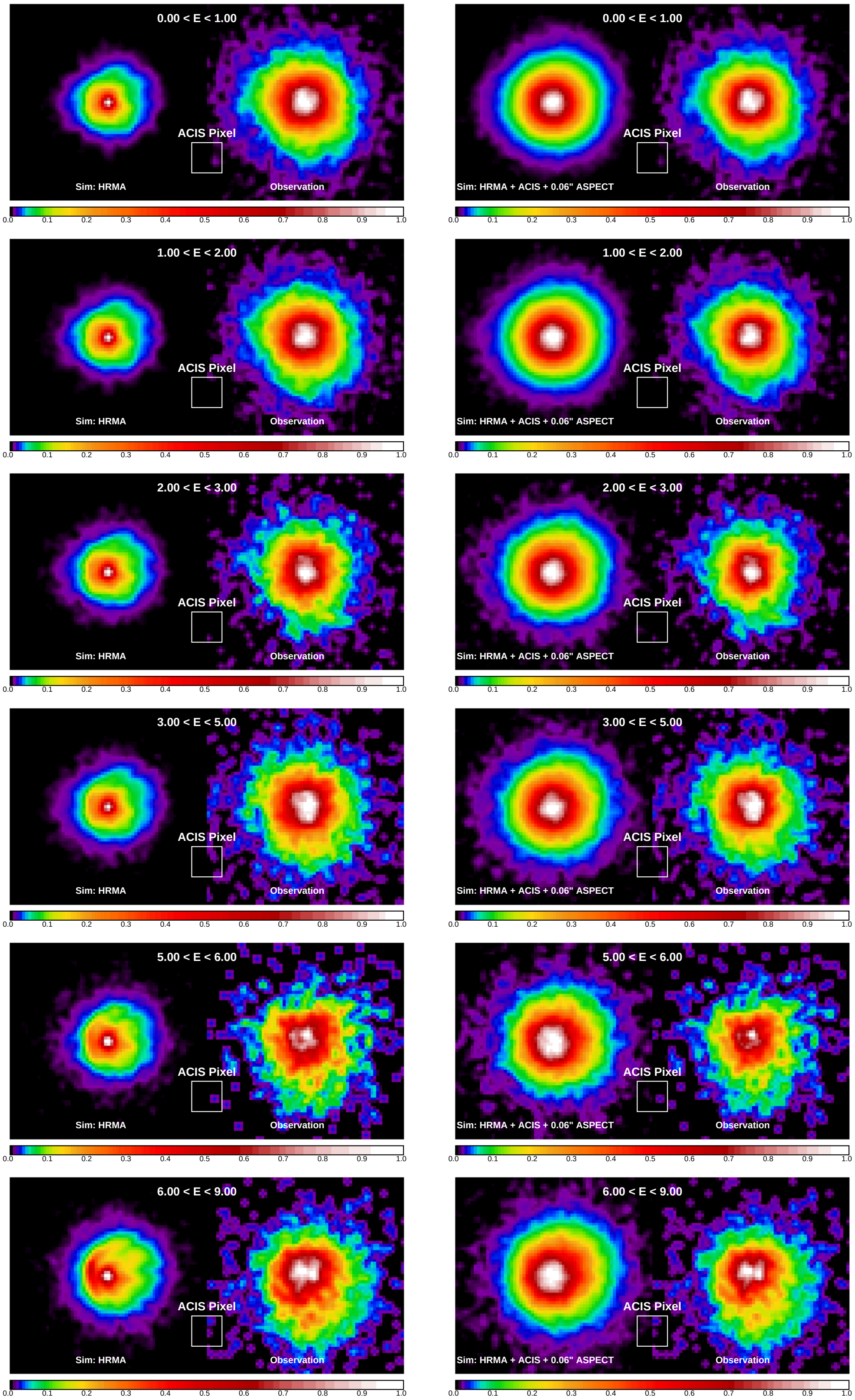

Figure 8. Comparisons of 2D PSFs for 7.7″ source. Left: model optic *vs.* data; Right: model telescope *vs.* data.

energy elongation of the source is in the same direction in both pointings, which is a good indication that it is a telescope effect and not an intrinsic feature of the single object in each pointing which contributes at those energies.

3. CONCLUSIONS

Analysis of the low-energy *Chandra* HRMA+HRC-I PSF shows our model to be in relatively good agreement with observations. Corroboration of this with observations with ACIS is not yet possible, as our detector and telescope dither models are not sufficiently accurate. For the first time we are able to examine the high-energy behavior of the PSF, and find that our models agree with it qualitatively, but with differences in the orientation of the elongations. Unfortunately, all of the high-energy data are obtained from ACIS-S+HETG observations, introducing unknown distortions in the PSF by the gratings.

At the beginning of the analysis of the ACIS data we had hoped to be able to put more quantitative limits on how the PSF varies with energy. However, the current crop of observations does not have enough signal to provide the statistics necessary to uniquely specify the PSF, and the deficiencies in our detector and telescope models prevent us from making quantitative predictions with the optics model.

ACKNOWLEDGMENTS

This work was supported by NASA Contract NAS8-39073.

REFERENCES

1. *The* Chandra *Proposers' Observatory Guide*, 5 ed., Dec. 2002. http://asc.harvard.edu/proposer/POG/.
2. D. Jerius, L. Cohen, M. Freeman, T. Gaetz, J. P. Hughes, D. Nguyen, W. A. Podgorski, M. Tibbetts, L. Van Speybroeck, and Z. P., "The Role of Modeling in the Calibration of Chandra's Optics," in *Proc. SPIE, Vol. 5165, X-Ray and Gamma-Ray Instrumentation for Astronomy XIII*, 2004. this volume.
3. D. Jerius, R. H. Donnelly, M. S. Tibbetts, R. J. Edgar, T. J. Gaetz, D. A. Schwartz, L. P. Van Speybroeck, and P. Zhao, "Orbital measurement and verification of the Chandra X-ray Observatory's PSF," in *Proc. SPIE Vol. 4012, p. 17-27, X-Ray Optics, Instruments, and Missions III, Joachim E. Truemper; Bernd Aschenbach; Eds.*, pp. 17–27, July 2000.
4. M. Juda, "Blur from Residual Errors in HRC Event Position Reconstruction," tech. rep., *Chandra* X-ray Observatory Center, Nov. 2001. http://hea-www.harvard.edu/ juda/memos/hrc_blur/hrc_blur.html.
5. D. Jerius, "Comparison of on-axis *Chandra* Observations of AR Lac to SOAsac Simulations," tech. rep., *Chandra* X-ray Observatory Center, Oct. 2002. http://asc.harvard.edu/cal/Hrma/psf/ARLac-onaxis.ps.
6. T. Aldcroft, "Image reconstruction performance," tech. rep., *Chandra* X-ray Observatory Center, Jan. 2001. http://asc.harvard.edu/mta/ASPECT/img_recon/report.html.

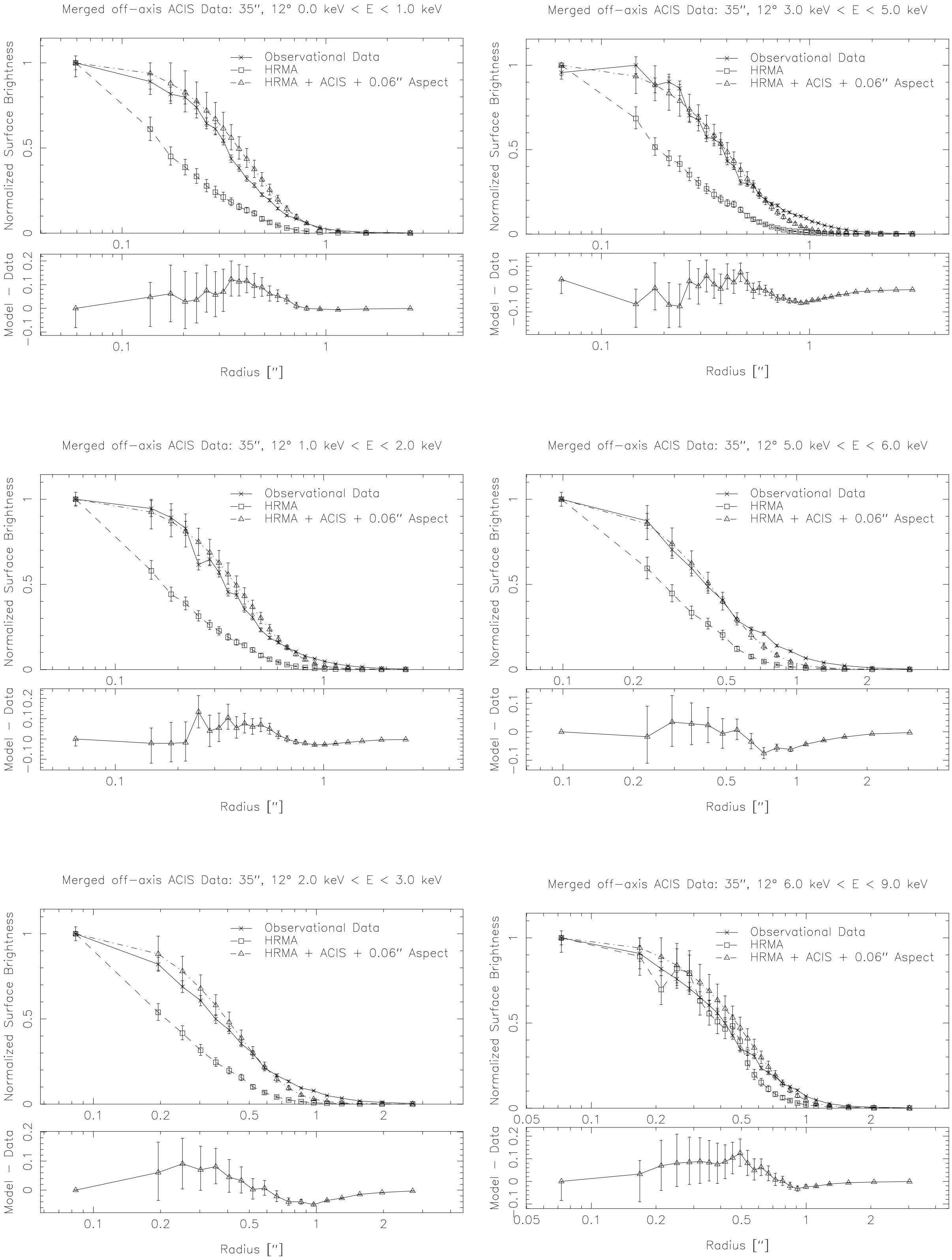

Figure 9. Comparisons of 1D PSFs for 35″ source.

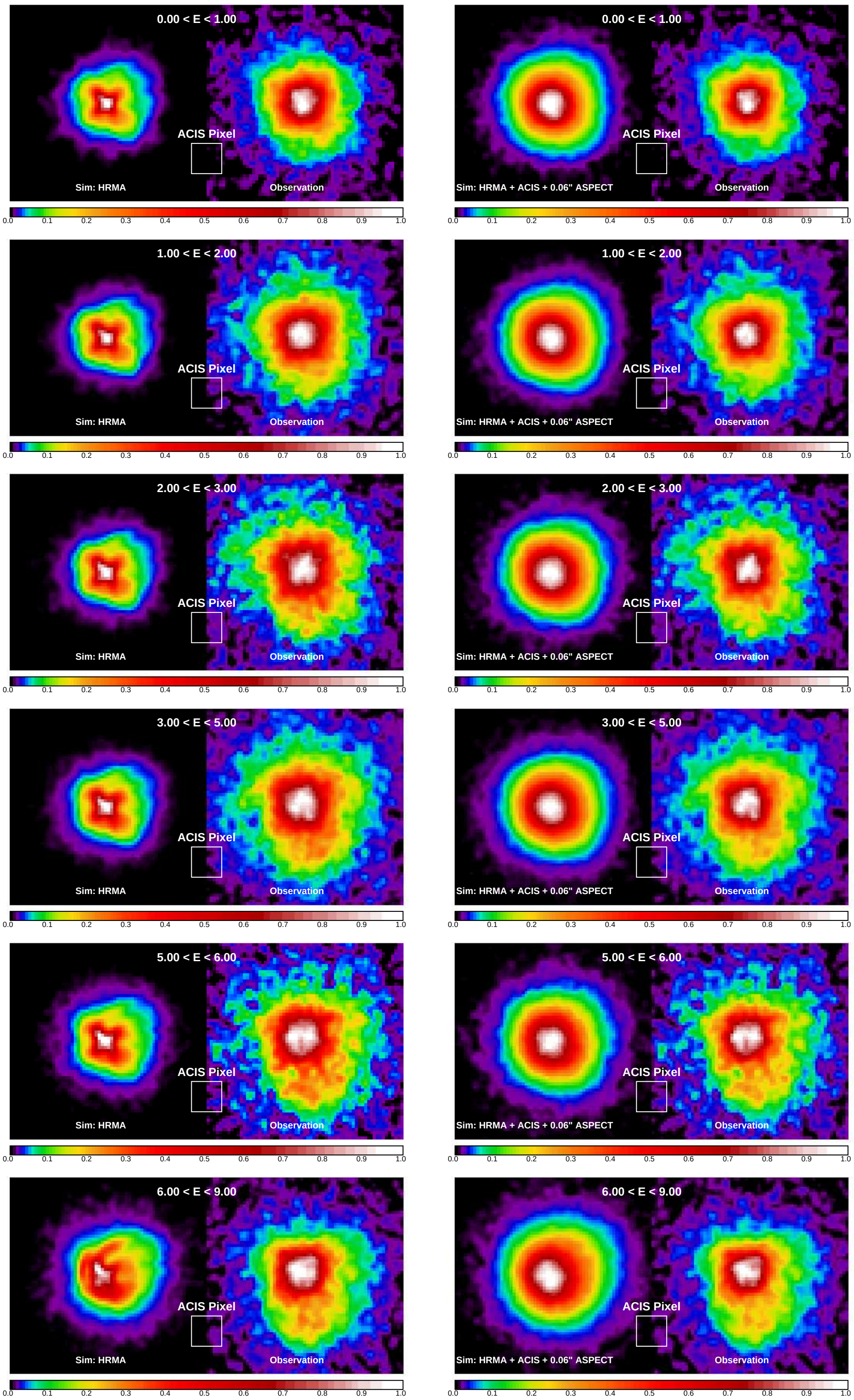

Figure 10. Comparisons of 2D PSFs for 35″ source. Left: model optic *vs.* data; Right: model telescope *vs.* data.